# THE ADIABATIC SOLUTION OF THE FEW-BODY INTEGRODIFFERENTIAL EQUATION

BY

RAPULA RONNY PHENYANE

# THE ADIABATIC SOLUTION OF THE FEW-BODY INTEGRODIFFERENTIAL EQUATION

by

RAPULA RONNY PHENYANE

submitted in accordance with the requirements for
the degree of

MASTER OF SCIENCE

in the subject

OF PHYSICS

at the

UNIVERSITY OF SOUTH AFRICA

SUPERVISOR : PROFESSOR G. J. RAMPHO

08 NOVEMBER 2021

# DECLARATION

Name: Rapula Ronny Phenyane

Student number: 57664404

Degree: Master of Science

THE ADIABATIC SOLUTION OF THE FEW-BODY INTEGRODIFFERENTIAL EQUATION.

I declare that the above dissertation is my own work and that all the sources that I have used or quoted have been indicated and acknowledged by means of complete references.

I further declare that I submitted the dissertation to originality checking software and that it falls within the accepted requirements for originality.

I further declare that I have not previously submitted this work, or part of it, for examination at UNISA for another qualification or at any other higher education institution.

SIGNATURE (R. R. Phenyane)

DATE

# Acknowledgments

I would like to thank my supervisor, Professor G. J. Rampho for his expert guidance, support and inspiration during the research related to this dissertation.

I thank my Mother, Mrs Clarah Phenyane and my sisters Victoria and Yvonne for their support and encouragement.

I thank Kathleen Julienne Cleophas, if it was not for her, I would not be here to conduct this research.

I also thank the members of the Department of Physics of the University of South Africa for their moral support.

 

# Summary

The original two-variable integrodifferential equation for few-body systems is modified by introducing boundary conditions in the radial and angular domains. The accuracy of the adiabatic approximation in solving this two-variable modified few-body integrodifferential equation is investigated. In this approximation the integrodifferential equation is decoupled into two single-variable equations for the radial motion and angular motion. The two equations are solved using the Lagrange-mesh methods. Ground-state energies of systems of particles interacting through realistic nucleon-nucleon and alpha-alpha interacting potentials and constituted by various numbers of particles are considered. The ground-state energies obtained are compared with those from the solution of the original two-variable integrodifferential equation as well as those obtain by other methods reported in the literature.

**Key Words** : Adiabatic approximation, Boundary conditions, Faddeev approach, Ground state energy, Integrodifferential equations, Hyperspherical harmonics, Lagrange-mesh method, Eigenvalue problem.

 

# Contents

# List of Figures

# List of Tables

# Chapter 1

# INTRODUCTION

The Schrödinger equation for many-body systems is very complex and cannot be solved exactly. There are several techniques used to simplify the equation for numerical implementation. The most popular technique in few-body physics is the Faddeev approach which transforms the many-body Schrödinger equation into a two-variable integrodifferential equation [1, 2]. The advantage of this equation is that it does not change form as the size of the system increases.

The two-variable integrodifferential equation for few-body systems is considered to be one of the most convenient methods employed in the analysis of few-body and many-body atomic and nuclear systems. This equation find its use in the studies of bound-state of nuclear system, such as system of $A$ identical bosons when two body correlation are taken into account, while disregarding higher order correlations [3, 4, 5]. The ground-state energies of systems of interest are determined either by solving the two-variable integrodifferetial equation directly or by means of a decoupling method, kown as Adiabatic approximation method [6].

The adiabatic approximation separate the two-variable integrodifferential equation into its radial and circular movements. For a given system of interest, the ground-state energies are determine by considering an adiabatic approximation scheme called the extreme adiabatic approximation, "EAA". Here, we regard the radial

movement to be fixed and use its radial position to determine the eigen-potential for the circular movement, which is then used to find the ground-state energies. This procedure gives us the lower limit of the binding energy [6, 7]. The upper limit of the binding energy is given by the uncoupled adiabatic approximation method, "UAA". The accuracy of the extreme adiabatic approximation is enhanced by the uncoupled adiabatic approximation method and this take place when we let the radial variables to be unfixed [7].

The Adiabatic Approximation found its origin in the approximations that were applied in atomic and molecular quantum mechanical systems. In atomic systems the main observations is that the circular speed of an electron is much higher in comparison to the radial speed of the nucleus [6, 7, 8, 9, 10]. As a result these two motions can be separated. This concept is applied to separate the two-integrodifferential equation. The Adiabatic approximation reduces many-variable differential equations into a system of coupled single-variable differential equation [6, 8, 10]. The main premise in adiabatic approximation is that the equations are separable in coordinates.

The adiabatic approximation appears to be well grounded for short range interacting nuclear systems, provided that the potentials that are involved display minimum changes at small distances [3]. In molecular interactions, the adiabatic approximation performs poorly because the potentials that are involved are over longer ranges. The down side of the adiabatic approximation is that it does not give precise outcome, even in nuclear interactions. The non-exact out comes are as a result of the type of the system potential to be solved, the decoupling of the radial and angular motion in the two-variable integrodifferential equation and by

the truncation of the domain [3]. Some of the information will inevitably be lost. Because of these facts, the adiabatic approximations will not be suitable at all times. As a result a reliable solution method is needed to examine its accuracy and to justify the continuing use of this approximation method in solving two-variable integrodifferential equations.

In this work we test the accuracy of the adiabatic approximation in solving the integrodifferential equation by using the Lagrange-Mesh method (LMM). The results are then compared with those obtained by the other methods reported in the literature. Because the Lagrange-mesh method is easy to use, give accurate results and it can be applied for simple quantum mechanical system [11, 12]. This method has been used with success to solve $^{12}C$ and $^{6}He$ nuclei defined as three body ($3\alpha$) and ($\alpha+n+n$) systems respectively, in hyper-spherical coordinates [13]. This gives confidence that Lagrange-mesh method will give correct results even when it is applied to the integrodifferential equation adiabatically for the first time in this work.

Lagrange-mesh method can be used to delineate both dynamic molecular or nuclear systems. It employs a set of Lagrange functions and the associated Gaussian quadrature defined on the grid. The Lagrange basis functions are an infinitely differentiable orthonormal set of functions that become naught at all coordinate points on a grid except one [11]. The Lagrange functions to be used in this work are the Lagrange-Laguerre and the Lagrange-Jacobi. The Lagrange-Laguerre are used to evaluate the radial part of our equation and the Lagrange-Jacobi are used for the angular part of the equation. However, the correctness of the LMM can be affected by faults in the Gauss quadrature which is brought in by the discontinuities in the potential [14]. This can be corrected by employing correct regularization

techniques.

The major goal of this work is to solve the two-variable integrodifferential equation of the extreme adiabatic approximation (EAA) by using the Lagrange-mesh method so that we can determine the ground state properties of some chosen nuclear systems. This is achieved by firstly expanding the wave function of the first EAA equation in terms of the Lagrange-Jacobi basis functions and when this expansion is substituted back into this equation, we obtain the eigenvalue problem in $z$, which we solve numerically to obtain the ground state eigen-potentials for fixed values of $r$. The second equation's wave function is also expanded in terms of the Lagrange Laguerre basis functions, and after substitution we obtain the second eigenvalue problem defined in $r$, in which the eigen-potential obtained from the first EAA equation is used to get the total ground-state energy of the system. The input potentials used in our calculations are the two-body interacting nucleon-nucleon potentials (NN) such as the Volkov, Baker and MTV which will be applied in a system of sizes, $3 \leq A \leq 7$. The degree of the hardness of the potential core for these potentials varies from Baker having the softest core, followed by the Volkov, with the MTV potential having the hardest core [3, 15]. We also test the validity of our solutions by using the Ali-Bodmer of the alpha-alpha ($\alpha - \alpha$) interacting potentials which is applied in larger systems, e.g the $^{12}C$, in which the interacting particles are grouped into alpha clusters of size $A\alpha$ [13]. In this instance, the $^{12}C$ nucleus can be regarded as a triple $\alpha$ system and be treated as a three-body system.

This dissertation is organized as follows: in Chapter 2 we present the formulation of the integrodifferential equation for A-body nuclear systems and show how this equation is decoupled adiabatically, by the extreme adiabatic approximation

 

(EAA) and by uncoupled adiabatic approximation (UAA). Chapter 3 is devoted to the Lagrange-mesh methods where we defined properties of Lagrange meshes and show how they are used to discretize the integrodifferential equation and its adiabatic equations. We then formulate the EAA eigenvalue problem to be treated numerically. Finally we present the results in chapter 5 and conclusion in chapter 6.

# Chapter 2

# INTEGRODIFFERENTIAL EQUATIONS

## 2.1 Few-body Integrodifferential Equations

In this section we detail the formulation of the two-body integrodifferential equations approach. The formulation is initiated by employing the Jacobi co-ordinates to do away with the influence of the center-of-mass of a system of $A$ interacting particles. Jacobi vectors $\boldsymbol{\eta}_a$ for this system, each with a position vector $\boldsymbol{y}_a$ are

defined by [1, 3]

$$\begin{cases} \boldsymbol{\eta}_N = \boldsymbol{y}_1 - \boldsymbol{y}_2 = \boldsymbol{r}_{12}, \\ \boldsymbol{\eta}_{N-1} = \sqrt{3}(\boldsymbol{y}_3 - \boldsymbol{Y}_3), \\ \vdots \\ \boldsymbol{\eta}_{N-a+1} = \sqrt{\frac{2}{a}(a+1)}(\boldsymbol{y}_{a+1} - \boldsymbol{Y}_{a+1}) = \sqrt{\frac{2a}{(a+1)}}(\boldsymbol{y}_{a+1} - \boldsymbol{Y}_a), \\ \vdots \\ \boldsymbol{\eta}_1 = \sqrt{\frac{2A}{A-1}}(\boldsymbol{y}_A - \boldsymbol{Y}), \\ \boldsymbol{Y_a} = \frac{1}{a}\sum_{b=1}^{a} \boldsymbol{y}_b, \qquad \boldsymbol{Y}_A = \boldsymbol{Y}, \end{cases} \tag{2.1}$$

where $\boldsymbol{Y}$ is the centre of mass. Note that the pair (1,2) is randomly chosen.

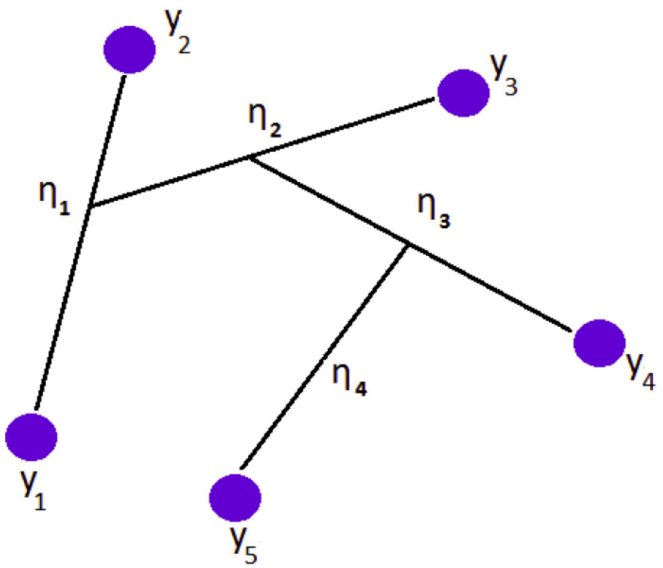


Figure 2.1: Some Jacobi vectors for a system of five particles.

The Schrödinger equation for the system is written as [3]

$$\left[\sum_{a=1}^{N}\frac{\hbar^2}{2m}\nabla^2_{\boldsymbol{\eta}_a}+V(\boldsymbol{\eta_1},...,\boldsymbol{\eta_N})-E\right]\Psi(\boldsymbol{\eta_1},...,\boldsymbol{\eta_N})=0 \tag{2.2}$$

where $m$ is the effective reduced mass, $V$ the total potential, $E$ the energy of the system and $\Psi$ the total wave function. If we assume that the interactions in the system are dominated by two particle interactions, then the interactions for $A$ particles can be described by

$$V(\boldsymbol{\eta}_1,...,\boldsymbol{\eta}_N)=\sum_{a<b}^{A}V(\boldsymbol{r}_{ab}). \tag{2.3}$$

The Faddeev equation for the total system have the form

$$(T-E)\,\psi_{ab}(\boldsymbol{\eta}_N)=-V(r_{ab})\Psi(\boldsymbol{\eta}_1,...,\boldsymbol{\eta}_N) \tag{2.4}$$

where the total wave function is decomposed in the form

$$\Psi(\boldsymbol{\eta}_1,...,\boldsymbol{\eta}_N)=\sum_{a<b\leq A}\psi_{ab}(\boldsymbol{\eta}_N) \tag{2.5}$$

where $\psi_{ab}(\boldsymbol{\eta}_N)$ are two-body amplitudes for the system. In order to solve equation (2.4) successfully one has to consider the particles number in the system in addition to two-body potentials applied as well as the hyper-spherical co-ordinates for each Jacobi vector $\boldsymbol{\eta}_a$. In less populated nuclear systems, two-body correlations play an important role. However as the number of particles in a system are increased, many-body correlation cannot be ignored. In order to distinguish between the

various correlations, we expand the total wave function as

$$\psi(\boldsymbol{y}) = \sum_{[L]=0}^{\infty} H_{[L]}(\boldsymbol{y})\Upsilon_{[L]}(r) \tag{2.6}$$

where $H_{[L]}(\boldsymbol{y})$ is a harmonic polynomial of degree $L$ in and $\Upsilon_{[L]}(r)$ is a function of a hyper-radius $r$ [3]

$$r = \left[\sum_{a=1}^{N} \eta_a^2\right]^{\frac{1}{2}} = \left[2\sum_{a=1}^{A} (\boldsymbol{y}_a - \boldsymbol{Y})^2\right]^{\frac{1}{2}} = \left[\frac{2}{A}\sum_{a<b\leq A} r_{ab}^2\right]^{\frac{1}{2}}. \tag{2.7}$$

and $[L]$ is a set of $3A-4$ quantum numbers of the system. The hyperspherical co-ordinate and the Jacobi vectors $\eta_a$ are related by [16]

$$\begin{cases} \eta_N = r\cos\phi_N \\ \eta_{N-1} = r\sin\phi_N\cos\phi_{N-1} \\ \eta_a = r\sin\phi_N ... \sin\phi_{a+1}\cos\phi_a, (\phi_1 = 0), \end{cases} \tag{2.8}$$

with the surface element $d\Omega$ given by [1]

$$d\Omega = dw_1 \prod_{b=2}^{N} (\sin\phi_b)^{3N-4} cos^2\phi_b d\phi_b dw_b \tag{2.9}$$

where $\phi_a$ is a set of the hyper-angles and $w_a$ angular coordinates of the Jacobi coordinate $\boldsymbol{\eta}_a$. For $b = N$, equation (2.9) can be written as

$$d\Omega = (\sin\phi_N)^{3N-4}\cos^2\phi_N d\phi_N dw_N d\Omega_{N-1}, \tag{2.10}$$

where $D = 3N$. We now express the volume element as

$$d^{3N}\eta = r^{D-1}drd\Omega, \tag{2.11}$$

using the surface element $d\Omega$ of the unit hypersphere $r = 1$ defined in $(D-3)$-dimensional space. If we let $r_{ab} = r\cos\phi$ and $z = \cos 2\phi = \frac{2r_{ab}^2}{r^2} - 1$ , we write the surface element as

$$\begin{aligned} d\Omega &= \frac{1}{2^{D/2}}(1-z_N)^{(3N-5)/2}(1+z_N)^{1/2}dz_N dw_N d\Omega_{N-1} \\ &= W(z)dz_N dw_N d\Omega_{N-1} \end{aligned} \tag{2.12}$$

where $W(z)$ is the weight function defined as [1]

$$W(z) = (1-z)^{(3A-8)/2}(1+z)^{1/2}. \tag{2.13}$$

The concept of hyper-central potential

$$V_0(r) = \frac{1}{h_0^{\alpha\beta}}\int_{-1}^{1} V(r_{ab})w(z)dz \tag{2.14}$$

incorporate many-body correlations. The hyper-central potential is given by the average of the two-body potentials in the system. Now equation (2.3) with $V_0(r)$ incorporated on both sides is written as [3]

$$\left|T + \frac{A(A-1)}{2}V_0(r) - E\right| \Upsilon_{ab}(\boldsymbol{y}) = -\left[V(r_{ab}) - V_0(r)\right]\Psi(\boldsymbol{y}). \tag{2.15}$$

The two-body amplitudes $\Upsilon_{ab}(\boldsymbol{y})$ has a Faddeev-like form for a set of $A$ particles interacting via a two-body potentials. In the case of central interactions we can write [17]

$$\Upsilon_{ab}(\boldsymbol{y}) = H^e_{[L]}(\boldsymbol{y})F^e(r_{ab}, r) \tag{2.16}$$

which leads to

$$\left[T + \frac{A(A-1)}{2}V_0(r) - E\right] H^e_{[L]}(\boldsymbol{y}) F^e(r_{ab}, r)$$
$$= -\Big[V(r)_{ab} - V_0(r)\Big] H^e_{[L]}(\boldsymbol{y}) \sum_{c<d\leq A} F^e(r_{cd}, r). \tag{2.17}$$

To get the solution of Eq.(2.17) we expand the wave function in terms of the potential harmonics basis and regularise in $r$ and $z$ coordinates in the form

$$F^e(r_{ab}, r) = r^{-(D-1)/2} w^{-1/2}(z) \sum_{a<b<A} P^e(z, r), \tag{2.18}$$

where the variable $z = \cos 2\phi = 2r^2_{ab}/r^2 - 1$ and $D = 3(A-1)$. We then project Eq.(2.17) on the $r_{ab}$ space to obtain the integrodifferential equation for $P^e(z, r)$ given as [3, 18]

$$\left[\frac{\hbar^2}{m}(\hat{T}_r - \frac{4}{r^2}\hat{T}_z) + \frac{A(A-1)}{2}V_0(r) - E\right] P^e(z, r) = -V^{e'}(z, r)\kappa(z, r), \tag{2.19}$$

where the kinetic energy operators have the form

$$\hat{T}_r = -\frac{\partial^2}{\partial r^2} + \frac{l_0(l_0+1)}{r^2}, \tag{2.20}$$

$$\hat{T}_z = \frac{1}{w_0(z)}\frac{\partial}{\partial z}(1-z^2)w_0(z)\frac{\partial}{\partial z}, \tag{2.21}$$

with $l_0 = (D-3)/2$ and $w_0(z) = (1-z^2)^{-1/2}$. The abbreviations

$$V^e(z, r) = V\Big(r\sqrt{\frac{1+z}{2}}\Big) - V_0(r), \tag{2.22}$$

$$\kappa(z,r) = P^e(z,r) + \int_{-1}^{1} f^e(z,z')P^{e'}(z',r)dz' \tag{2.23}$$

are used. Note that in the traditional integrodifferential equations approach only $\hat{T}_r$ is regularised and

$$\hat{T}_z = \frac{1}{w_0(z)}\frac{\partial}{\partial z}(1-z^2)w_0(z)\frac{\partial}{\partial z}, \tag{2.24}$$

Here, $f^e(z,z')$ is a projection function, which projects other interacting pairs, say $(cd)$, into the pair of interest $(ab)$ [3, 17]. The projection function is given in terms of Jacobi polynomials $P_n^{\alpha,\beta}$ as

$$f^e(z,z') = w_\mu(z')\sum_n P_n^{\alpha,\beta}(z)P_n^{\alpha,\beta}(z')\frac{(f_n^2-1)}{h_n^{\alpha,\beta}}, \tag{2.25}$$

where

$$h_n^{\alpha,\beta} = \int_{-1}^{+1}\left[P_n^{\alpha,\beta}(z)\right]^2 w_\mu(z)dz \tag{2.26}$$

is the normalization constant of the Jacobi polynomial. The factors $(f_n^2-1)$, are related to the particle that are connected to the pair $ab$ and those that are disconnected to the pairs $ab$. These factors have the form

$$f_n^2 = \left[2(A-2)P_n^{\alpha,\beta}(-1/2) + \frac{(A-2)(A-3)}{2}P_n^{\alpha,\beta}(-1)\right]\frac{1}{P_n^{\alpha,\beta}(1)}, \tag{2.27}$$

for identical particles, where $2(A-2)$ and $(A-2)(A-3)$ is the number of connected and disconnected pairs, respectively, in a A-body system [3, 4, 17].

## 2.2 Adiabatic Approximation Method

The adiabatic approximation (AA) is used to solve the Schrödinger equation by separation of variables [6, 7, 8]. This approximation is also known as Born-Oppenheimer approximation (BOA) which is used to solve energies of molecular systems, whereby the angular motion of the electrons is decoupled from the radial motion of the nucleus [6, 10]. The light electron which is considered to move faster, is used to find the effective potential for the much slower and heavier nucleus at a fixed distance $r$. This effective potential is then used in another equation to find the energy of the system [17].

We can solve the two-variable integrodifferential equation adiabatically by assuming that the orbital motion is very fast as compared to the radial motion and posses most of the energy of the system [1]. This results in an integrodifferential equations in $z$ and $r$ variables. For the extreme adiabatic approximation (EAA) the amplitude is expressed as the product [3, 4]

$$P^e(z,r) = P^e_\lambda(z,r)u_\lambda(r), \tag{2.28}$$

where $P^e_\lambda(r,z)$ is assumed to vary weakly with $r$ and is a solution of one variable integrodifferential equation in $z$ for all fixed values of $r$. The integrodifferential equation in equation (2.19) is then split into two equations. The first equation is given by [15]

$$\frac{4\hbar^2}{mr^2}T_z P^e_\lambda(z,r) + V^e(z,r)\kappa_\lambda(z,r) = U^e_\lambda(r)P^e_\lambda(z,r) \tag{2.29}$$

where $U^e_\lambda(r)$ are eigen-potential associated with eigen-amplitudes $P^e_\lambda(z,r)$. The

eigen-potential $U_\lambda(r)$ in equation (2.29) are evaluated for fixed hyper-radial positions $r$ and the resulting outcomes are then substituted into the radial equation (the second EAA equation) stated as

$$\left[\frac{\hbar^2}{m}\left[-\frac{d^2}{dr^2}+\frac{l_0(l_0+1)}{r^2}\right]+\frac{A(A-1)}{2}V_0(r)+U_\lambda^{e'}(r)-E_\lambda^{EAA}\right]u_\lambda^e(r)=0, \quad (2.30)$$

to get the binding energy $E_\lambda^{EAA}$ of the system. The wave function of this adiabatic approximation scheme is now specified as

$$\psi_{EAA}(z,r)=u_\lambda(r)/r^{3A/2-2}\sum_{a<b\leq A}P_\lambda^e(z,r). \quad (2.31)$$

We now pay attention to a complete changing of $r$ in $P_\lambda^e(r,z)$. These lead us to another scheme of the adiabatic approximation known as the uncoupled adiabatic approximation "UAA" [19, 20]. The adiabatic approximation results in the upper limit of the exact binding energy. To include this variations, we presuppose $\psi_{EAA}(z,r)$ to be variational solution and present the eigen-functions in the form [3]

$$B_\lambda(r,\Omega)=\sum_{a<b\leq A}P_\lambda^e(\frac{2r_{ab}^2}{r^2}-1,r), \quad (2.32)$$

where the normalizing constant of $B_\lambda(r,\Omega)$ is expressed as

$$\int \mid B_\lambda(r,\Omega)\mid^2 d\Omega=\langle B_\lambda \mid B_\lambda\rangle=1, \quad (2.33)$$

for every chosen values of $r$, where $d\Omega$ forms a surface of the unit hypersphere. The wave function of a complete adiabatic uncoupling is now stated as

$$\psi(x)=B_\lambda(r,\Omega)u_\lambda(r)/r^{3A/2-2}. \quad (2.34)$$

The radial equation for the (UAA) is derived by expressing equation (2.30) in the form

$$\int d\Omega B_\lambda^*(r,\Omega)\left\{\frac{\hbar^2}{m}\left[-\frac{d^2}{dr^2}+\frac{l_0(l_0+1)}{r^2}\right]+\frac{A(A-1)}{2}V_0(r)+U_\lambda^{e'}(r)-E\right\}B_\lambda(r,\Omega)u_\lambda(r)=0, \tag{2.35}$$

which result in

$$\left\{\frac{\hbar^2}{m}\left[-\frac{d^2}{dr^2}+\frac{l_0(l_0+1)}{r^2}\right]+\frac{A(A-1)}{2}V_0(r)+U_\lambda^{e}(r)-\frac{\hbar^2}{m}\left\langle B_\lambda\middle|\frac{d^2B_\lambda}{dr^2}\right\rangle-E_\lambda^{UAA}\right\}u_\lambda^{UAA}(r)=0, \tag{2.36}$$

where the orthogonality relation of $B_\lambda$ and $dB_\lambda/dr$ has been used. From the relation

$$\left\langle B_\lambda\middle|\frac{d^2B_\lambda}{dr^2}\right\rangle=-\left\langle\frac{dB_\lambda}{dr}\middle|\frac{dB_\lambda}{dr}\right\rangle \tag{2.37}$$

we can show that the effective potential of "UAA" in equation (2.36) is always positive if we use the right hand side of equation (2.37) in equation (2.36). The outcome is that the ground-state energies derived from both adiabatic approximation procedures will result in $E_\lambda^{UAA}$ being greater than $E_\lambda^{EAA}$ at all times. This proof the basic inequality [15, 21]

$$E_{EAA}\leq E_{exact}\leq E_{UAA} \tag{2.38}$$

and it is worth noting that when solving the original two-variable integrodifferential equation adiabatically, the exact binding energy can be estimated accurately by the interpolation formula given by [15]

$$E_{exact}\simeq E^{UAA}+0.2(E^{EAA}-E^{UAA}). \tag{2.39}$$

However in this work we only determine the ground-state energies of the modified

integrodifferential equation in equation (2.19) by the extreme adiabatic approximation (EAA). These energies will be compared to exact energies found using equation (2.39) and energies calculated using other methods reported in the literature.

# Chapter 3

# THE LAGRANGE-MESH METHOD

## 3.1 Fundamentals

In general, the integral of a function $f(y)$ defined in the interval $(p, q)$ can be approximated by the Gaussian quadrature

$$\int_p^q f(y)w(y)dy \approx \sum_{a=1}^{N} w_a f(y_b), \tag{3.1}$$

where $y_a$ are the abscissae involving N roots of an orthogonal polynomials of degree $N$

$$p_N(y_a) = 0. \tag{3.2}$$

and $w_a$ are the weights associated with these polynomials [11, 12]. Several types of Gauss quadrature exist and their applications depends on a specific interval being used. For example, the Gauss-Laguerre quadrature whose properties are used to construct $r$-dependent Lagrange function, are based on the Laguerre polynomials which are orthonormal with respect to weight function $w(x) = y^{\alpha}e^{-y}$ and are defined in the interval $[0, \infty)$. The Gauss-Jacobi quadrature, whose properties are also used in this work to construct $z$ -dependent Lagrange functions, are defined in the finite interval $[-1, 1]$.

In the Lagrange-mesh method, integrals are evaluated using the Gauss quadrature approximation by [11]

$$\int_p^q g(y)dy \approx \sum_{a=1}^{N} \lambda_a g(y_a) \tag{3.3}$$

where $g(y)$ is a real function and $\lambda_a$ are the weights of the quadrature given by

$$\lambda_a = \frac{w_a}{w(y_a)}. \tag{3.4}$$

A set of Lagrange functions $f_a(y)$ have the property [11]

$$f_a(y_b) = \lambda_a^{-1/2}\delta_{ab}, \tag{3.5}$$

where $\delta_{ab}$ is the Kronecker delta function. The Gauss quadrature for the overlap integral has the form

$$\langle f_a \mid f_b \rangle = \int_p^q f_a(y) f_b(y) dy = \langle f_a \mid f_b \rangle^G = \delta_{ab}. \tag{3.6}$$

The property (3.3) indicates that each of the Lagrange functions $f_a(y)$ vanish at all grid points except at $y_a$.

The Lagrange functions provide a variational basis that leads to the Hamiltonian matrix elements being constructed using Gauss approximation. We demonstrate this by considering a one-dimensional Schrödinger equation

$$H\psi = -\frac{\hbar^2}{2m}\frac{d^2\psi(y)}{dy^2} + V(y)\psi = E\psi(y) \tag{3.7}$$

where $\psi(y)$ is the wave function, $V(y)$ a scalar potential and $E$ the energy of the

system. The variational wave function is the approximated by

$$\psi(y) = \sum_{b}^{N} c_b f_b(y), \tag{3.8}$$

with a set of $N$ Lagrange functions $f_b(y)$ defined in the interval $[p, q]$. This involves grid points $y_b$ for $b = 1, 2, 3, ..., N$ and variational parameters $c_b = \lambda_b^{1/2}\psi(y_b)$.

Substituting the expansion (3.8) in the Schrödinger equation, multiplying by $f_a(y)$ and integrating over the whole domain leads to a set of coupled algebraic equations

$$\sum_{b=1}^{N} \big[T_{ab} + V_{ab}\big] c_b = E c_a \tag{3.9}$$

where $T_{ab}$ and $V_{ab}$ are the kinetic energy and potential matrix elements. The kinetic energy matrix elements are calculated as

$$T_{ab} = \langle f_a \mid T \mid f_b \rangle = -\int_p^q f_a(y) \frac{d^2}{dy^2} f_b(y) dy = -\int_p^q f_a(y) f_b^{''}(y) dy \tag{3.10}$$

for $\hbar = 2m = 1$, which can be approximated by Gaussian quadrature as [12]

$$T_{ab} \approx T_{ab}^G = -\sum_{k=1}^{N} \lambda_k f_a(y_k) f_b^{''}(y_k) = -\lambda_a^{1/2} f_b^{''}(y_b). \tag{3.11}$$

The Gauss approximation matrix elements of the potential $V(y)$ are represented by [11]

$$V_{ab} = \langle f_a \mid V \mid f_b \rangle = \int_p^q f_a(y) V(y) f_b(y) dy \tag{3.12}$$

and leads to

$$V_{ab} \approx V_{ab}^G = \sum_{k=1}^{N} \lambda_k f_a(y_k) V(y_k) f_b(y_k) = \int_p^q f_a(y) V(y) f_b(y) dy = V(y_a)\delta_{ab}. \tag{3.13}$$

When equations (3.11) and (3.13) are implemented in equation (3,9) we get [11]

$$\sum_{b=1}^{N}\big[-\lambda_a^{1/2}f_b''(y_a)+V(y_a)\delta_{ab}\big]c_b=Ec_a. \tag{3.14}$$

The features of equation (3.14) show that it depends only on the values of the approximated kinetic and potential energy matrix at given grid points $y_b$ and not on individual Lagrange functions. Let us introduce the scaling factor $h$ which is responsible for reducing the infinite domain to a finite domain of interest so that the new Lagrange functions reads [11]

$$f_b(y)=h^{-1/2}f_b(y/h). \tag{3.15}$$

The revised eigenvalue equation (3.14) transforms to

$$\sum_{b=1}^{N}\big[-h^{-2}\lambda_a^{1/2}f_b''(y_a)+V(hy_a)\delta_{ab}\big]c_b=Ec_a. \tag{3.16}$$

The number of mesh points $N$ and the value of the scaling factor $h$ affect the accuracy of the results of calculated energies.

## 3.2 The Lagrange Functions

To approximate the solution of equation (2.19), we employ the Lagrange basis functions. These are special functions that are infinitely differentiable and are orthogonal at the Gauss approximation points [11]. Lagrange functions used here are the Lagrange-Laguerre and Lagrange-Jacobi basis functions.

### 3.2.1 Lagrange-Laguerre functions

Lagrange-Laguerre mesh points are based on Lagrange polynomials $L_N^\sigma(r)$ which are orthogonal over the interval $[0,\infty)$ with respect to the weight function

$$w(r) = r^\sigma e^{-r}, \tag{3.17}$$

where $\sigma$ is a real parameter [11]. The Lagrange-Laguerre mesh is given by [11]

$$L_N^\sigma(r_a) = 0 \tag{3.18}$$

where $r_a$ $(a = 1, 2, 3, ...N)$ are the zeros of the Laguerre polynomials of order N. The standard Lagrange-Laguerre basis functions are defined by [22]

$$f_a(r) = (-1)^i r_a^{1/2} (h_N^\sigma)^{-1/2} r \frac{L_N^\sigma(r)}{r - r_a} r^{\frac{\sigma}{2}} e^{\frac{-r}{2}} \tag{3.19}$$

where

$$h_N^\sigma = \frac{\Gamma(\alpha + N + 1)}{N!} \tag{3.20}$$

is the normalization constant of the Laguerre polynomials. The matrix elements of the radial kinetic energy operator $T = -\partial^2/\partial r^2$ are given by [14, 22]

$$T^r_{aa'} = \left\langle f_a(r) \left| \frac{-d^2}{dr^2} \right| f_{a'}(r) \right\rangle \tag{3.21}$$

$$= \begin{cases} -(1)^{a-a'} \frac{(r_a + r_{a'})}{\sqrt{r_a r_{a'}}(r_a - r_{a'})^2} & ; \quad a \neq a' \\ -\frac{1}{12} + \frac{2N+\sigma+1}{6r_a} + \frac{-(\sigma-2)(\sigma+2)}{12r_a^2} & ; \quad a = a' \end{cases} \tag{3.22}$$

where $\sigma = 3A - 5$ [22]. The centrifugal and Coulombic matrix terms, have singularities at $r = 0$ which result in errors in the Gauss quadrature. To circumvent

this problem the Lagrange-Laguerre functions are regularised to suppress the singularity [11].

### 3.2.2 Lagrange-Jacobi functions

The Lagrange-Jacobi functions are determined from the Jacobi polynomials $P_M^{\alpha,\beta}(z)$, which are orthogonal over the interval $[-1,+1]$ with respect to the weight function

$$w(z) = (1-z)^{\alpha}(1+z)^{\beta} \tag{3.23}$$

where $\alpha, \beta > -1$ [11]. The Lagrange-Jacobi mesh points $(z_b)$ are chosen such that

$$P_M^{\alpha,\beta}(z_b) = 0, \tag{3.24}$$

where the $z_b$ are the zeros of the Jacobi polynomial of order $M$ [11]. In this work we make use of the Lagrange-Jacobi functions regularized by $(1-z^2)^{\mu/2}$ [11, 14], where $\mu$ is the regularizing parameter. The regularized Lagrange-Jacobi functions are defined as [23]

$$O_b(z) = (-1)^{N-b}\sqrt{\frac{(1-z)^{\alpha+\mu}(1+z)^{\beta+\mu}}{(2N+\gamma)(1-z_b^2)^{\mu-1}(h_N)}}\frac{P_N^{\alpha,\beta}(z)}{z-z_b} \tag{3.25}$$

where

$$h_N = \frac{2^{\gamma}}{\gamma+2N}\frac{\Gamma(\alpha+N+1)\Gamma(N+\beta+1)}{N!\Gamma(\gamma+N)} \tag{3.26}$$

is the normalization constant of the Jacobi polynomial and $\gamma = \alpha+\beta+1$. The parameters $(\alpha,\beta)$ define the Lagrange-Jacobi functions and for this work are set to $(\alpha,\beta) = (\alpha_0,\beta_0)$ with $\alpha_0 = 3A/2-4$ and $\beta_0 = 0.5$. The matrix elements of the

parametric angular kinetic operator is given by [23]

$$T^z_{bb'} = \left\langle O_b(z)\middle|\left[(1-z^2)\frac{d^2}{dz^2} - z\frac{d}{dz}\right]\middle|O_{b'}(z)\right\rangle \tag{3.27}$$

$$= \begin{cases} (-1)^{b-b'}\left[\frac{(2\mu-1)z_b}{(z_b-z_{b'})} - \frac{2(1-z_b^2)}{(z_b-z_{b'})^2}\right]\left(\frac{(1-z_b^2}{1-z_{b'}^2}\right)^{(\mu-1)/2} & ; \quad b \neq b' \\ -\frac{1-(2N+\gamma)^2}{12} + \frac{\omega_I+\omega_{II}z_b+(\omega_{III}z_b^2)}{6(1-z_b^2)} & ; \quad b = b' \end{cases} \tag{3.28}$$

where $\omega_I = \alpha^2+\beta^2-6\mu+4, \omega_{II} = \alpha^2-\beta^2$ and $\omega_{III} = 6(\mu-1)^2$. Matrix elements for all the scalar functions calculated with $f_a(r)$ and $O_b(z)$ are diagonal.

## 3.3 Matrix Eigenvalue Problem

In this section we make use of properties of the Lagrange-Laguerre and Lagrange-Jacobi basis function to construct the eigen-value problem for solving the integrodifferential equation directly and adiabatically. To solve the integrodifferential equation directly we begin by expressing the two-body amplitude $P^\alpha(z,r)$ as a linear combination of Lagrange basis functions [11]

$$P^e(z,r) = \sum_{a=1}^{N}\sum_{b=1}^{M} C_{ab} f_a(r) O_b(z) \tag{3.29}$$

where $C_{ab}$ are the variational parameters given by

$$C_{ab} = (\lambda_a\lambda_b)^{1/2} P^e(r_a, z_b). \tag{3.30}$$

We apply the expanded wave function into equation (2.19), multiply the right hand side by

$$P^{e*}(r,z) = f_{a'}(z)O_{b'}(r) \tag{3.31}$$

and integrate over the problem domain. This lead to the eigenvalue problem given by

$$\sum_{a'=1}^{N}\sum_{b'=1}^{M}\left[\frac{\hbar^2}{h^2 m}\left(T^r_{aa'}\delta_{bb'} + \frac{4}{r_a^2}T^z_{bb'}\delta_{aa'}\right) + V_{aa',bb'}\right]C_{a'b'} = EC_{ab} \tag{3.32}$$

where $V_{aa',bb'}$ are the potential matrix elements and $T^r_{aa'}(T^z_{bb'})$ are the radial (angular) kinetic energy matrix elements. Here were use the Gauss quadrature approximation of the kinetic energy matrix elements. The matrix elements for the the potential $V_{aa',bb'}$ and calculated as

$$V_{aa',bb'} = V^e(r_a, z_{b'})\left(\delta_{bb'} + (\lambda_b\lambda_{b'})^{1/2} f^e(z_{b'}, z_b)\right)\delta_{aa'} \tag{3.33}$$

Using the properties of equations ( 3.19) and (3.25) we get a modified eigenvalue problem [11, 14, 23]

$$\sum_{a'=1}^{N}\sum_{b'=1}^{M}\left[\frac{1}{h^2}H^e_{ab,a'b'} + V^e(hr_a, z_{b'})\left(\delta_{bb'}\delta_{aa'} + \sqrt{\lambda_b\lambda_{b'}}f^e(z_{b'}, z_b)\delta_{aa'}\right)\right]C_{a'b'} = EC_{ab} \tag{3.34}$$

used to solve the integrodifferential equation directly. The Hamiltonian $H^e_{ab,a'b'}$ is given by

$$H^e_{ab,a'b'} = \frac{\hbar^2}{m}\left[T^r_{aa'}\delta_{bb'} - \frac{4}{r_a^2}\left(T^z_{bb'} - \frac{1}{16}\delta_{bb'}\right)\delta_{aa'}\right]. \tag{3.35}$$

where the matrix elements $T^r_{aa'}$ and $T^z_{bb'}$ are also dependent on parameters $\alpha, \beta$ and $\mu$.

Similarly the matrix eigenvalue equations for solving equation (2.19) with the

extreme adiabatic approximation EAA, which is the focus of this work, are express as

$$\sum_{b'=1}^{N_z}\left[H^z_{bb'}+V^e(hr_a,z_{b'})\left(\delta_{bb'}+\sqrt{\lambda_b\lambda_{b'}}f^{e'}(z_{b'},z_b)\right)\right]C_{b'}=U^e_k(hr_a)C_b \tag{3.36}$$

where

$$H^z_{ab}=-\frac{4\hbar^2}{mh^2r_a^2}T^z_{bb'}. \tag{3.37}$$

Equation (3.36) is used to calculate the eigen-potential $U^{e'}_k(hr_a)$ of the system, which is then used in

$$\sum_{a'=1}^{N_r}\left[-\frac{\hbar^2}{mh^2}T^r_{aa'}+\left(\frac{\hbar^2}{4mh^2r_a^2}+U^{e'}_\lambda(hr_a)\right)\delta_{aa'}\right]C_{a'}=EC_a \tag{3.38}$$

to determine the energy of the system. The parameters $(h,\lambda_a,\lambda_b,\mu,,\alpha)$ which define the matrix elements $T^r_{aa'}$ and $T^z_{bb'}$ in equation (3.36) and (3.38) are the same as those in equation (3.34).

# Chapter 4

# RESULTS AND DISCUSSION

Calculations presented requires values of the input parameters; $h, \mu, \alpha, \beta$ and the zeros of the Jacobi and Laguerre polynomials. These parameters need to be optimised in order to obtain reasonable values for the ground-state energies. The Gaussian quadrature weights and grid points where constructed with the accuracy of about $3 \times 10^{-14}$ [24]. In our calculations the parameter $\mu$, the regulation parameter , was set to $\mu = -0.5$. The parameters of the Jacobi function $(\alpha, \beta)$ which are related to the eigenfunctions of the angular kinetic energy operator where set to $(\alpha, \beta) = (\alpha_0, \beta_0)$. The scaling factor parameter $h$ which is determined by the hyperradial range of the total potential of the system [25] and is defined as $h = r_m/r_N$. Where $r_m$ is the range of the hypercentral potential and $r_N$ is the largest zero of the Laguerre polynomial. For this work $r_m = 20fm$ was used for three-body problems and $r_m = 30fm$ for many-body systems, i.e A = 4, 5, 6 and 7. The mass parameter $\hbar^2/m$, where $m$ is the nucleon's mass, depends on the type of the potential used as input in our calculations, either as nucleon-nucleon potentials (NN) or alpha-alpha potential $(\alpha - \alpha)$.

## 4.1 Interaction Potentials

In this work, calculations are performed using two-body nucleon-nucleon (NN) and $\alpha - \alpha$ potentials. For the NN potentials we consider the Barker [26], Volkov

[27], Malfliet-Tjon MTV [28] potentials. For the $\alpha - \alpha$ interactions we employ Ali-Bodmer potential [29]. These potentials are widely used in studies of various nuclear systems which enable us to compare our work with other well known method used to solve nuclear problems. These potentials are briefly discussed below.

The Volkov and Barker potentials are both smooth and spin-independent potentials of the Gaussian form [8, 15]. The Barker potential, which has a more softer and finite attractive core [26, 30, 31, 32] is given as

$$V_B(r) = -E_0 e^{-(r/R)^2} \tag{4.1}$$

where $E_0 = 51.5$ MeV represent the depth of the potential and the interacting range, $R = 1.6$fm. On the other hand the Volkov potential is of the form

$$V(r) = E_A e^{-(r/R_A)^2} + E_B e^{-(r/R_B)^2} \tag{4.2}$$

where $E_A$, $E_B$ represent constants of the attractive and repulsive part of the potential [27]. The parameter values for the Volkov potential are specified in Table 4.1.

Table 4.1: Parameter values for the Volkov potential.

| $E_A[MeV]$ | $E_B[MeV]$ | $R_A[fm]$ | $R_B[fm]$ |
|---|---|---|---|
| 144.86 | -83.34 | 0.82 | 1.60 |

The MTV potential is a hard core potential is given by [9, 28]

$$V(r) = -\frac{E_A}{r} e^{-rR_A} + \frac{E_B}{r} e^{-rR_B}. \tag{4.3}$$

Where $E_A$, $E_B$, $R_A$ and $R_B$ are constants. The values for these parameters are specified in Table 4.2.

Table 4.2: Parameter values for the MTV potential.

| $E_A[MeV]$ | $E_B[MeV]$ | $R_A[fm]$ | $R_B[fm]$ |
|---|---|---|---|
| 578.09 | 1458.05 | 1.550 | 3.110 |

The Ali-Bodmer is a soft core $\alpha\alpha$ potential given by [29, 31]

$$V(r) = E_A e^{-r^2 R_A^2} - E_B e^{-r^2 R_B^2} \tag{4.4}$$

used to describe cluster interaction in nuclei. Again, where $E_A$, $E_B$, $R_A$ and $R_B$ are constants. The values of these parameters are specified in specified in Table 5.3 [29].

Table 4.3: Parameter values for the Ali-Bodmer potential.

| $E_A[MeV]$ | $E_B[MeV]$ | $R_A[fm]$ | $R_B[fm]$ |
|---|---|---|---|
| 500 | 130 | 0.70 | 0.475 |

## 4.2 Three-body Systems

In this section we present results for a three body system. Many other studies on this nuclear system are available in the literature which makes the comparison possible. The input potentials are the NN potentials discussed in the previous section. The ground state energies are calculated using the parameters, $r_{max} = 20$ fm and $\frac{\hbar^2}{m} = 41.467$ MeV.fm$^{-2}$. We start by looking at the form of the effective potential $V_{eff}(r)$ for different potentials for the three-body system shown in Figure

4.1. The effective adiabatic potential is given by the relation

$$V_{eff}(r) = \frac{l_0(l_0+1)}{r^2} + U^e_{EAA}(r) \tag{4.5}$$

for the various two-body potentials. It is important to note that our calculations use the lowest adiabatic eigen-potential.

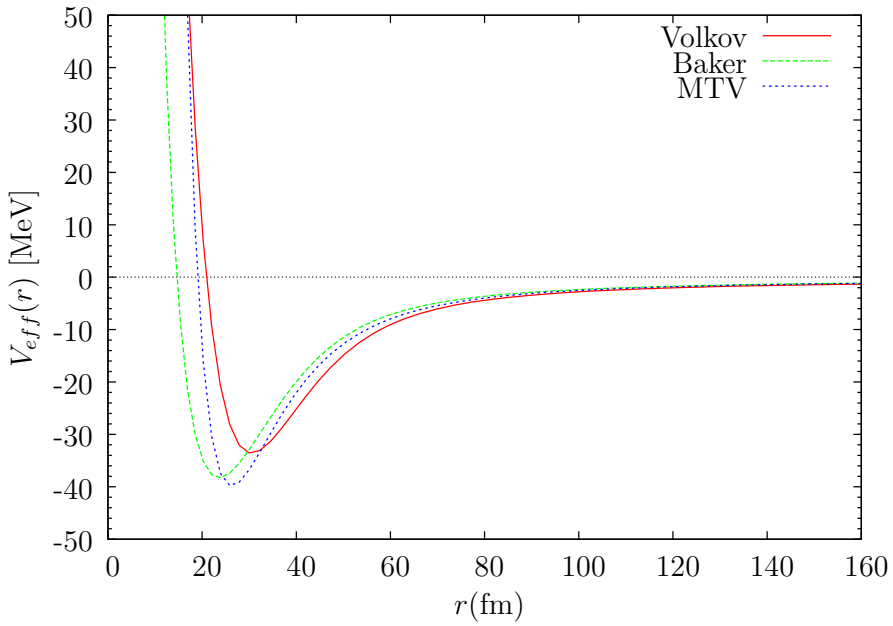


Figure 4.1: A plot of the effective potentials $V_{eff}(r)$ for three-body systems of the Baker ,Volkov and MTV potentials.

We notice from the figure tat the Barker potential exhibit the least hard core, followed by the Volkov, while MTV potential show the hardest core. This means that the degree of repulsiveness of the potential cores at small values of $r$, with Baker showing the weakest repulsion and MTV potential presenting the strongest repulsive core, which is expected to give the lowest binding energy compared to other NN potentials used.

We calculate the ground state energy for increasing grid sizes $M_z$ and $N_r$. We

limit our calculations to cases of equal radial and angular bases sizes $N_r = M_z$. The results are given in in Table 4.4 and Figure 4.5 (a)-(c). The convergence was tested up to the grid size of $N_r = N_z = 70$ which was enough to give reasonable results. As can be seen in the table and the figures, the ground-state energies converge with increasing sizes of the grid to the values $-9.840MeV$, $-8.575MeV$, and $-8.343MeV$ for the Barker, Volkov and MTV potentials respectively. The Barker and Volkov potentials results converge rapidly to their respective energies while the hard core MTV potential results convergence slowly.

Table 4.4: Convergence of the ground-state energies $E_0$ as a function of mesh sizes $N^2 = N_r \otimes M_z$ for 3-body-systems using various NN potentials.

| | $E_0[MeV]$ | | |
|---|---|---|---|
| N | Volkov | MTV | Baker |
| 10 | -8.712450 | -9.966646 | -9.855020 |
| 20 | -8.574763 | -8.475398 | -9.840471 |
| 30 | -8.574774 | -8.370699 | -9.840472 |
| 40 | -8.574775 | -8.353265 | -9.840471 |
| 50 | -8.574774 | -8.347483 | -9.840471 |
| 60 | -8.574773 | -8.344853 | -9.840471 |
| 70 | -8.574773 | -8.343439 | -9.840471 |

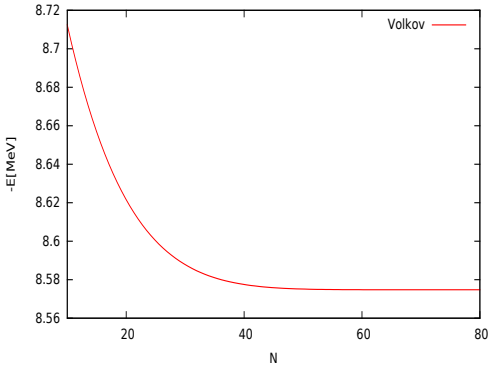


(a) Volkov

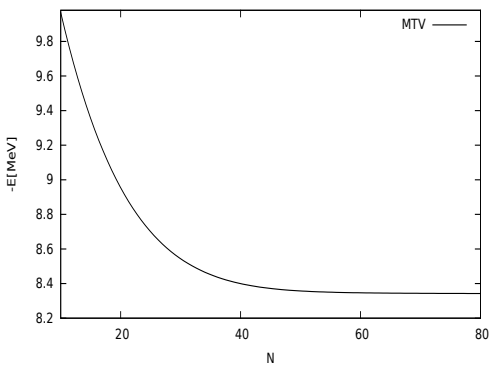


(b) MTV

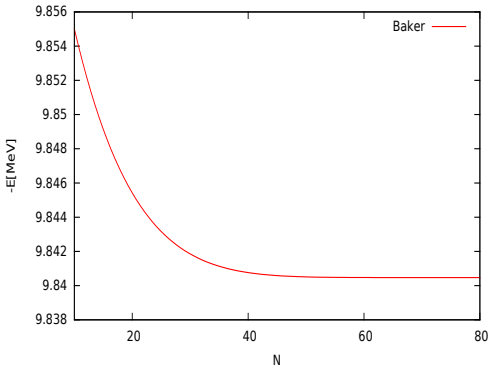


(c) Baker

Figure 4.2: A plot of ground-state energies as function of the basis sizes for the various NN potentials in 3-body system.

The ground-state energies calculated at grid size of $N_r = M_z = 70$ are compared with the results from the literature and are shown in Table 4.5. The results for this work are compared with those obtained with direct solution for few-body integrodifferential equation on Lagrange mesh [14], hyperspherical harmonics (HH) [33, 34], Born-Oppenheimer approximation (BOA) [6, 8, 35] and the S-state Integrodifferential Equation (SIDE) [5, 36]. It can be seen that our results are closely to those reported in the literature, with average percentage differences of about 1.5%, 3.9% and 0.84% for the Volkov, MTV and Baker potentials respectively. This accuracy is very impressive considering the simplicity of the integrodifferential equation.

Table 4.5: The ground-state energies for 3-body system obtained using the Volkov, MTV and Baker potentials.

| $E_0[MeV]$ | | |
|---|---|---|
| Volkov | MTV | Baker |
| -8.5748 | -8.3434 | -9.8405 |
| -8.4309[14] | -7.541[36] | -9.7386[8] |
| -8.44[5] | -8.2525[1] | -9.7812[6] |
| -8.4648[34] | -8.2527[37] | -9.7547[35] |

## 4.3 Many-body Systems

In this section, we calculate ground-state energies for A-body system (A = 4, 5, 6, 7) in s-state and observe the effect as the size of the system is increased. We start by calculating the ground-state energy for the four-body system and show the plots for the effective adiabatic potential ($V_{eff}$) of the Volkov, Baker and MTV potentials. Later, we show the results for $A > 4$ systems using Volkov, MTV and Ali-Bodmer potentials. Unless otherwise stated, we use the values $\frac{\hbar}{m} = 41.47$ MeV.fm $^{-2}$ and $r_{max} = 30$fm as input parameters in our calculations.

### 4.3.1 The NN potential

The plots of the effective potential for A = 4 using Baker, Volkov and MTV potentials are shown in Figure 4.6. Comparing with Figure 4.1 in the previous section, we notice a general increase in the depth of the potentials as the system size is increased to A = 4. The Baker potential shows a much deeper well while MTV potential shows the most repulsion barrier.

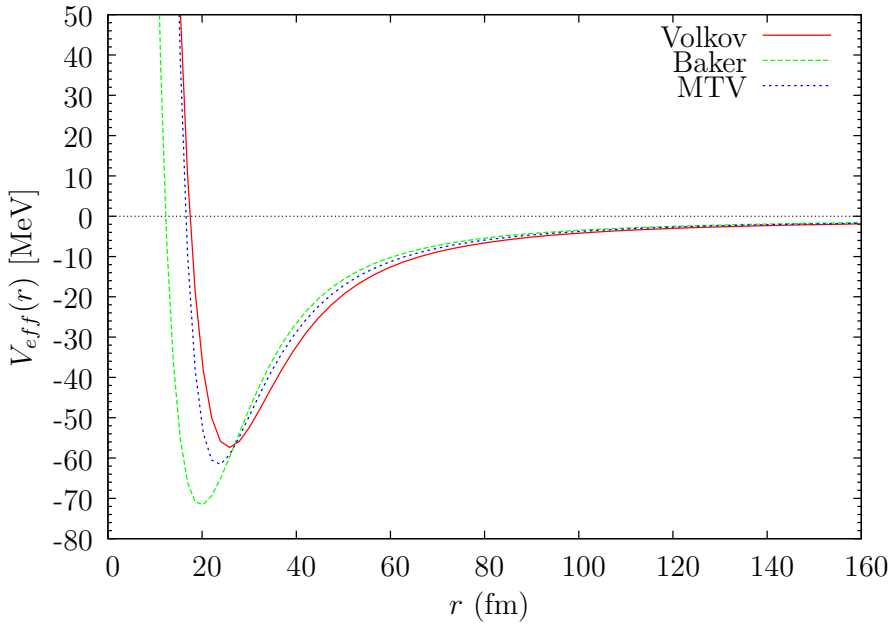


Figure 4.3: A plot of the effective potential $V_{eff}(r)$ for the 4-body system obtained with various NN potentials.

The plots of the effective adiabatic potentials as a function of radial distance for A = 4, 5, 6 and 7 for the Volkov potential are shown in Fig 4.7. We notice an increase in the depth and the repulsion barrier of the potentials as A increases. This explains the decrease in the ground state energy as the system size increases.

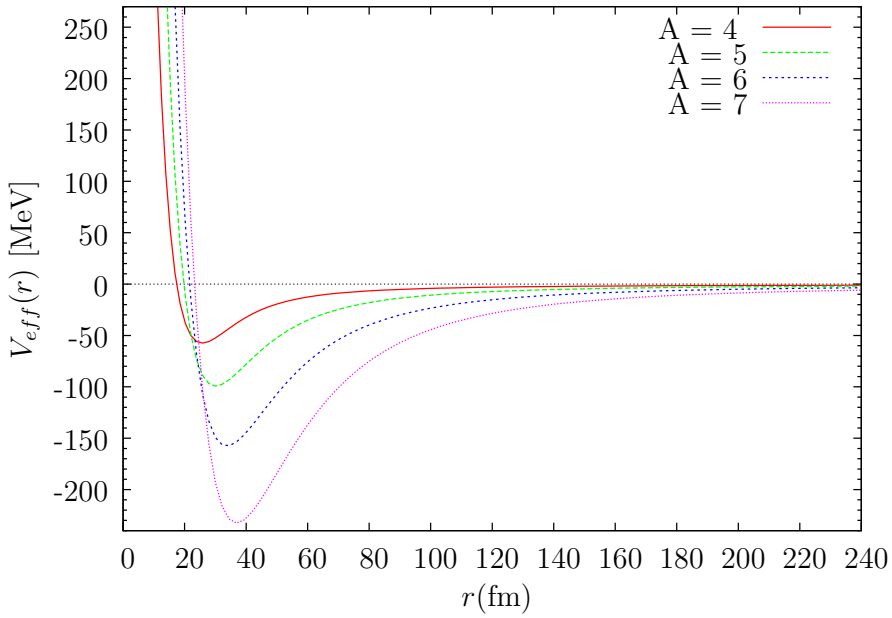


Figure 4.4: A plot of the effective potential $V_{eff}(r)$ for the A = 4, 5, 6 and 7 system for the Volkov potential.

The convergence of the ground-state energies for A = 4 - 7 with increasing basis sizes for the Volkov potential are given in in Table 4.8. As before, we limit our calculations for the cases of equal radial and angular bases sizes $N_r = M_z$ for values of up to $N_r = N_z = 70$. The convergence is reached at $N = 30$. The summary of the ground-state energies for A = 4, 5, 6, 7 together with those from the literature for the Volkov potential are shown in Table 4.9. Our results are close to those obtained using the Hyperspherical Harmonics expansion (HH) [2, 38], with the percentage differences of 3.7%, 1.6% and 0.6% for the four-body, five-body and six-body systems, respectively. For the seven-body system with the Volkov potential, our results deviate from those reported in [38] by 3.6%.

Table 4.6: Convergence of the ground-state energies $E_0$ as a function of mesh size $N^2 = N_r \otimes N_z$ for the A = 4, 5, 6, 7 systems using the Volkov potential.

| | E [MeV] | | | |
|---|---|---|---|---|
| N | A = 4 | A = 5 | A = 6 | A = 7 |
| 10 | -30.313274 | -71.035138 | -119.219823 | -181.366965 |
| 20 | -29.129999 | -67.173009 | -122.001259 | -193.480284 |
| 30 | -29.130150 | -67.171661 | -122.006994 | -193.451930 |
| 40 | -29.130155 | -67.171661 | -122.006994 | -193.451930 |
| 50 | -29.130156 | -67.171662 | -122.006994 | -193.451930 |
| 60 | -29.130156 | -67.171662 | -122.006994 | -193.451930 |
| 70 | -29.130156 | -67.171662 | -122.006994 | -193.4519300 |

Table 4.7: The ground-state energies $E_0$ for the A = 4 -7 system obtained using the Volkov potential.

| | $E_0[MeV]$ | | |
|---|---|---|---|
| A = 4 | A = 5 | A = 6 | A = 7 |
| -29.130 | -67.172 | -122.007 | -193.452 |
| -30.25[2, 37] | -68.28[2] | -122.78[2] | 200.13[38] |
| -30,40[6] | -61.0[14] | -111.06[14] | - |
| -26.47[14] | - | - | - |

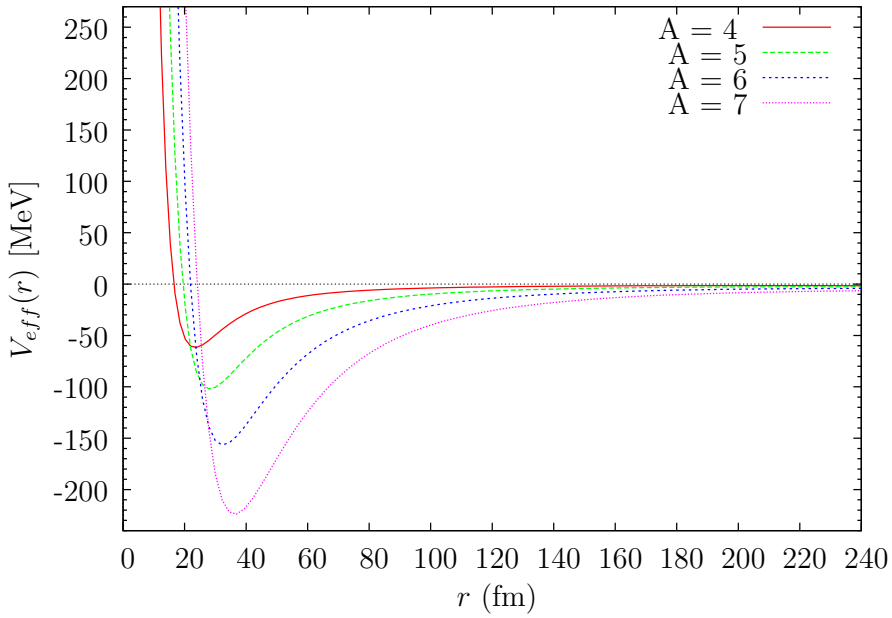


Figure 4.5: A plot of the effective potential $V_{eff}(r)$ for A = 4, 5, 6 and 7 systems for the MTV potential.

The plots of the effective adiabatic potentials for A-body systems (A = 4, 5, 6, 7) for the MTV potential are shown in Figure 4.5. We notice an increase in the depth of the potential with increasing size of the system. The convergence of the ground-state energies for the MTV potential with increasing basis sizes is shown in Table 4.8. The convergence seems to be slow for all system sizes using the MTV potential. The ground-state energies calculated with $N = 70$ are summarised Table 4.9. Our results are in good agreement with those obtained using the Faddeev method [18, 39, 40]. The percentage difference is 5.5% [18] for A = 4 and 0.75% [39] for A = 6.

Table 4.8: Convergence of the ground-state energies $E_0$ as a function of mesh sizes $N^2 = N_r \otimes N_z$ for the A = 4, 5, 6, 7 systems using the MTV potential.

| | E [MeV] | | | |
|---|---|---|---|---|
| N | A = 4 | A = 5 | A = 6 | A = 7 |
| 10 | -32.459561 | -80.823796 | -139.622163 | -214.681609 |
| 20 | -29.265598 | -66.984867 | -119.966635 | -187.196183 |
| 30 | -29.040132 | -66.338577 | -118.378902 | -183.787023 |
| 40 | -28.987111 | -66.178844 | -117.983938 | -182.944655 |
| 50 | -28.966990 | -66.117457 | -117.831993 | -182.620952 |
| 60 | -28.957375 | -66.087974 | -117.759020 | -182.465644 |
| 70 | -28.952089 | -66.071721 | -117.718812 | -182.380149 |

Table 4.9: The ground state binding energies $E_0$ for the A = 4 -7 system obtained using the MTV potential.

| $E_0[MeV]$ | | | |
|---|---|---|---|
| A = 4 | A = 5 | A = 6 | A = 7 |
| -28.952 | -66.072 | -117.719 | -182.380 |
| -30.63[18] | - | -116.84[39] | - |
| -30.25[37] | - | - | - |
| -30.40[3] | - | -116.48[40] | - |

### 4.3.2 The Ali-Bodmer Potential

When a nuclear system become very large such as $^{12}C$ and $^{16}O$ we resort to treat it as $\alpha$ interacting systems of size A $\alpha$, where A represent the number of $\alpha$ particles in the system. For example, a $^{12}C$ nucleus can be regarded as the triple ( $3\alpha$) system where each alpha particle act as point like boson interacting by means of $\alpha - \alpha$ effective forces [13]. For this work we calculate ground-state energy for the A $= 3\alpha, 4\alpha, 5\alpha, 6\alpha, 7\alpha$ systems. We use $r_{max}$ = 30fm and the mass constant $\frac{\hbar^2}{m}$ = 10.367 MeV.fm$^{-2}$ as input parameters. The convergence of the ground-state energy is checked against increasing basis sizes up to $N = 70$ and the results are given in Table 4.10. We notice a good convergence with increasing bases sizes. However the convergence becomes slow as the system size (A$\alpha$) increases.

Table 4.10: Convergence of the ground-state energies $E_0$ as a function of mesh sizes $N^2 = N_r \otimes N_z$ for the $A = 3, 4, 5, 6, 7$ systems for the Ali-Bodmer potential.

| | E [MeV] | | | | |
|---|---|---|---|---|---|
| N | A = 3 | A = 4 | A = 5 | A = 6 | A = 7 |
| 10 | -6.772766 | -8.733464 | -12.381644 | -18.615673 | -23.760345 |
| 20 | -4.610363 | -8.170327 | -11.561459 | -14.902300 | -18.124662 |
| 30 | -4.607015 | -8.170073 | -11.557964 | -14.885122 | -18.109291 |
| 40 | -4.602723 | -8.170071 | -11.557953 | -14.885153 | -18.109811 |
| 50 | -4.599035 | -8.170071 | -11.557953 | -14.885152 | -18.109797 |
| 60 | -4.596073 | -8.170071 | -11.557953 | -14.885152 | -18.109797 |
| 70 | -4.597738 | -8.170071 | -11.557953 | -14.885152 | -18.109797 |

A comparison of the ground-state energies with those from the literature are given in Table 4.11. Our results for the $3\alpha$ system agrees with those obtained for using the Faddeev and the Hyperspherical harmonics expansion methods [14, 41, 42], with percentage differences of about 10.0%. However, for systems bigger than $3\alpha$ our results deviate from those reported in the literature. This requires investigation.

Table 4.11: Ground-state energies $E_0$ of A$\alpha$ body system obtained using the Ali-Bodmer potentials.

| $E_0[MeV]$ | | | | |
|---|---|---|---|---|
| A = 3 | A = 4 | A = 5 | A = 6 | A = 7 |
| -4.5977 | -8.1700 | -11.5580 | -14.8852 | -18.1098 |
| -5.12[41, 42] | -11.07[44] | -16.22[44] | -20.13[44] | - |
| -5.13[43] | -11.10[45] | - | - | - |

We show the plots of the effective potential $V_{eff}(r)$ for the Ali-Bodmer potential for the A$\alpha$ systems. Figure 4.6 shows an increase in the depth and the repulsion barrier of the potential as the size of the system increases, which correspond to what is being reported in the literature [31].

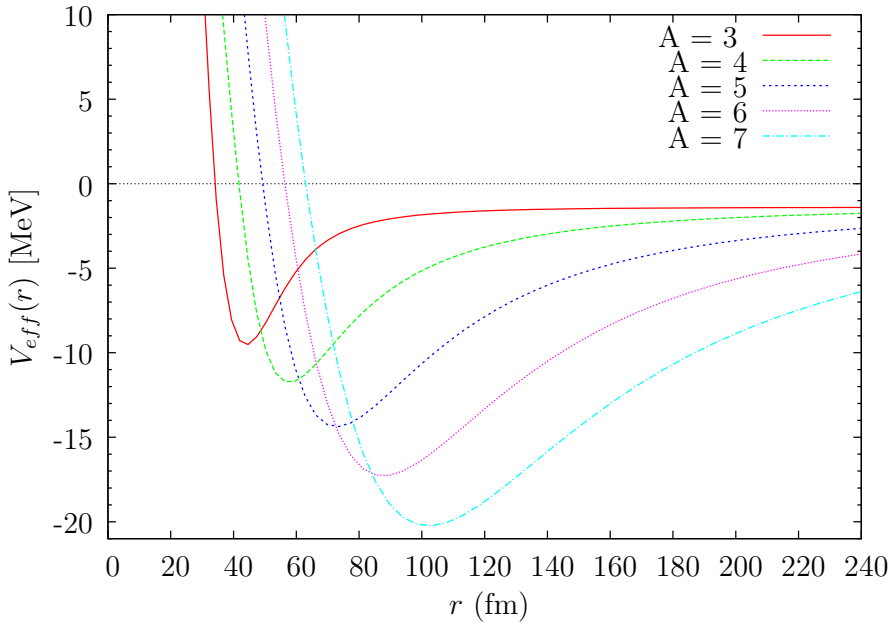


Figure 4.6: A plot of the effective potential $V_{eff}(r)$ for A = 4, 5, 6 and 7 for the Ali-Bodmer potential.

# Chapter 5

# CONCLUSION

In this work we investigated the accuracy of the Adiabatic Approximation (AA) in solving the few-body integrodifferential equation. The resulting adiabatic equations were solved using the Lagrange-mesh method. The adiabatic approximation method separate the integrodifferential equation into two variables $r$ and $z$, which is based on the assumption that the angular part of the equation contribute more to the overall interaction of the system than the radial part. This results in two equations of the so called extreme adiabatic approximation EAA, where the first equation is in $z$ coordinates and is used to find a specific eigen-potentials $U_\lambda(r)$ for fixed values of $r$. Then the calculated eigen-potential is then substituted in the the radial equation of the EAA, to find the binding energy. This gives the lower bound of the binding energy. The matrix elements of these equations were constructed using the regularised the Lagrange-Laguerre and Lagrange-Jacobi functions. The resulting eigenvalue problem has a structure that depends on the mesh points, quadrature weights and specific parameters that needed to be optimised in order to ensure a good convergence of the calculated energies. We have investigated the convergence of the ground-state energies with increasing grid sizes, and restricted our calculations to cases of equal basis sizes $N_r = M_z = 70$.

Our results for a three-body system are overall in good agreement with those reported in the literature. The ground-state energies results for the MTV hard core

potential have on average a 3.9% difference to those reported in the literature. The results for Volkov potential show an average deviation of about 1.48%. The Baker potential ground-state energies for a three-body system has a percentage difference of 0.83%. Ali-Bodmer potential for $3\alpha$ system shows overall deviation of about 11.0%.

Furthermore, we applied the method to system of $A = 4, 5, 6, 7$ constituents for the Volkov, MTV and Ali-Bodmer potentials. The results converged rapidly and consistently for all results of the systems. The calculated ground-state energies for all the systems and for all potentials are remarkably close to those generated by sophisticated methods, reported in the literature. These demonstrates that the adiabatic approximation provides a reliable method of constructing ground-state solutions for few-body systems described by the two-variable integrodifferential equation.

We have verified that the adiabatic approximation generate very accurate ground-state solutions for few-body integrodifferential equation. The results obtained are comparable with those reported in the literature obtained using very sophisticated state-of-the-art methods. Moreover, the solution method, the Lagrange-mesh method, is very simple and easy to implement. However the true accuracy of the adiabatic approximation will be determined from the direct solution of the integrodifferential equation. This work is on going and will be reported elsewhere.

# Bibliography


[1] M. Fabre de la Ripple, M. Braun and S. A. Sofianos: Prog. Theor. Phys. **98**(6), 1261 (1997).

[2] M. Gattobigio, A. Kievsky and M. Viviani: Phys. Rev. **C 83**(2), 024001.1 (2011).

[3] M. Fabre de la Ripelle, H. Fiedeldey and S. A. Sofianos: Phys. Rev. **C 38**(1), 449 (1988).

[4] S. A. Sofianos, G. J. Rampho, and R. M. Adam: Phys. Part. Nucl **40**(6), 757 (2009).

[5] M. Fabre de la Ripelle: *Few-body syst.* **20**(3), 129 (1996).

[6] T. K. Das and H. T. Coelho: Quim. Nov. **11**, 1 (1998).

[7] V. P. Brito, H. T. Coelho and T. K. Das: Rev. Bras. Fis. **21**(2), 309 (1991).

[8] T. K Das, H. T. Coelho and V. P. Brito: Phys. Rev. **C 48**(5) 2201 (1993).

[9] J. G. Zabolitzky, K. E. Schmidt, and M. H. Kalos: Phys. Rev. **C 25**, 1111 (1982).

[10] S. K. Adhikari, V. P. Brito, H. T. Coelho and T. K Das: IL Nuo. Ci. **B 107**(1) 77 (1992).

[11] D. Baye: Phys. Rep. **565**, 1 (2015).

[12] D. Baye: J. Phys. B: At. Mol. Opt. Phys. **28**, 4399 (1995).

[13] P. Descouvemont and C. Daniel: Phys. Rev. **C 67**, 044309 (2003).

[14] G. J. Rampho: J.Phys, Conf. Ser **915**, 012005 (2017).

[15] J. L. Ballot, M. Fabre de la Ripelle and J. S. Levinger: Phys. Rev. **C 26**, 2301 (1982).

[16] M. Fabre de la Ripelle: Ann. Phys. (NY), **147**, 231 (1983).

[17] R. M. Adam and H. Fiedeldey: J. Phys. G: Nucl. Part. Phys. **19**, 703 (1993).

[18] R. M. Adam, S. A. Sofianos, H. Fiedeldey and M. Fabre de la Ripelle: J. Phys. **G 18**, 1365 (1992).

[19] T. K. Das, H. T. Coelho and M. Fabre de la Ripelle: Phys. Rev. **C 26**, 2281 (1982).

[20] J. H. Macek: J. Phys. **B 1**, 831 (1968).

[21] M. F. Fabre de la Ripelle and H. Fiedeldey and S.A. Sofianos: *Few-Body Syst.*, **6**, 157 (1989).

[22] M. Beiner, M. Fabre de la Ripelle: Nuov. Cim. Let. **1**, 584 (1971).

[23] G. J. Rampho: Math. Theor. **49**, 295202.1 (2016).

[24] W. H. Press, S. A. Teukolsky , W. T. Vetterling and B. P. Flannery: *Numerical Recipes in FORTRAN (2nd Ed.): The Art of Scientific Computing* (New York, USA: Cambridge University Press), (1992).

[25] H. Masui, S. Aoyama and D. Baye: Prog. Theor. Exp. Phys. **A02**, 123A02 (2013).

 

[26] G. A. Baker et al: Phys. Rev. **125**, 1754 (1962).

[27] A. B. Volkov: Nucl. Phys. A **74**, 33 (1965).

[28] R. E. Malet and J. A. Tjon: Nucl. Phys. **A 127**, 161.1 (1969).

[29] S. Ali and A. Bodmer: Nucl. Phys. **80**, 99 (1966).

[30] M. Fabre de la Ripelle, H. Fiedeldey, and S. A Sofianos: *Supplements to Research Report* edited by T. Sasakawa *et al.* (Tohoku I.R. University Press, Sendai), **19** 360 (1986).

[31] M. Lekala, S. A. Sofianos, R. M. Adam and V. B. Belyaev: *Alpha-particle within Nuclei*, Researchgate. net, publication, 257444806 (2012)

[32] Yu. A. Simonov: Proceedings of the International Symposium on the Present Status and Novel Developments in the Nuclear Many-body problems, Rome, Edited by F. Calogero and C. Ciofi degli Atti (Editrice Compositori, Bolonga ), 527 (1972).

[33] G. L. Payne, J. L. Friar and B.F Gibson, I. R. Afnan: Phys. Rev. C **22**, 823 (1980).

[34] G. J. Rampho, L. C. Mabunda and M. Ramantswana: J. Phys: Conf. Series. **905**, 012037 (2017).

[35] T. K. Das, H. T. Coelho and M. Fabre de la Ripple: Phys. Rev. **C 26**(5) 2281 (1992).

[36] W. Oehm, S. A. Sofianos, H. Fiedeldey and M. Fabre de la Ripelle: Phys. Rev. **C 42**(6), 2322 (1990).

[37] K. Varga and Y. Suzuki: Phys. Rev. **C 52**, 2885,1 (1995).

[38] T. K. Das and R. Chattopadhyay: Fizika **B 2**, 262 (1993).

 

[39] B. Mukero : Msc Dissertation: University of South Africa, (2012).

[40] N. Barnea and M. Viviani: Phys. Rev. **C 61**, 034003 (2000).

[41] Dithlase Frans Masita: Msc Dissertation: University of South Africa, (2006).

[42] E. M. Tursunov et al: Nucl. Phys. **A 723**, 365 (2003).

[43] I. Filikhin, V. M. Suslov and B. Vlahovic: J. Phys. G: Nucl. Part. Phys **31**, 1207 (2005).

[44] K. Varga and Y. Suzuki: Phys. Rev. **C 52**, 2885.1 (1995).

[45] O. A. Yakubovskii: Sov. J. Nucl. Phys. **5**, 937.1 (1967).

 